Anais da Academia Brasileira de Ciências
ISSN: 0001-3765
aabc@abc.org.br
Academia Brasileira de Ciências
Brasil

SIMÃO, ANDRÉ G.; GUIMARÃES, LUIZ G.
Tunneling effects in resonant acoustic scattering of an air bubble in unbounded water
Anais da Academia Brasileira de Ciências, vol. 88, núm. 2, abril-junio, 2016, pp. 765-790
Academia Brasileira de Ciências
Rio de Janeiro, Brasil

Anais da Academia Brasileira de Ciências (2016) 88(2): 765-790
(Annals of the Brazilian Academy of Sciences)
Printed version ISSN 0001-3765 / Online version ISSN 1678-2690
http://dx.doi.org/10.1590/0001-3765201620150403
www.scielo.br/aabc

Tunneling effects in resonant acoustic scattering of an air bubble in unbounded water

ANDRÉ G. SIMÃO[1] and LUIZ G. GUIMARÃES[2]

[1]Departamento de Educação e Ciências - Núcleo de Física,
Instituto Federal de Educação Ciência e Tecnologia do Sudeste de Minas Gerais,
Rua Bernardo Mascarenhas, 1283 - Fábrica, 36080-001 Juiz de Fora, MG, Brasil
[2]Programa de Engenharia Oceânica/COPPE, Universidade Federal do Rio de Janeiro/UFRJ,
Centro de Tecnologia, Bloco C, Cidade Universitária, Ilha do Fundão,
Caixa Postal 68508, 21945-970 Rio de Janeiro, RJ, Brasil

Manuscript received on July 21, 2015; accepted for publication on November 27, 2015

ABSTRACT

The problem of acoustic scattering of a gaseous spherical bubble immersed within unbounded liquid surrounding is considered in this work. The theory of partial wave expansion related to this problem is revisited. A physical model based on the analogy between acoustic scattering and potential scattering in quantum mechanics is proposed to describe and interpret the acoustical natural oscillation modes of the bubble, namely, the resonances. In this context, a physical model is devised in order to describe the air water interface and the implications of the high density contrast on the various regimes of the scattering resonances. The main results are presented in terms of resonance lifetime periods and quality factors. The explicit numerical calculations are undertaken through an asymptotic analysis considering typical bubble dimensions and underwater sound wavelengths. It is shown that the resonance periods are scaled according to the Minnaert's period, which is the short lived resonance mode, called breathing mode of the bubble. As expected, resonances with longer lifetimes lead to impressive cavity quality Q-factor ranging from 10^{10} to 10^{5}. The present theoretical findings lead to a better understanding of the energy storage mechanism in a bubbly medium.

Key words: Acoustic Scattering, Minnaert Resonance, Semi-Classical Methods, Whispering Gallery Modes, Mie and Rayleigh Scattering.

1 - INTRODUCTION

The problem of resonant acoustic scattering by air filled spherical cavity in a infinite liquid medium, so-called single air bubble in water, is one of those famous problems in classical physics. Many scientists have

Correspondence to: Luiz Gallisa Guimarães
E-mail: lgg@peno.coppe.ufrj.br /
lula@if.ufrj.br

devoted effort and time to find intriguing properties of this ubiquitous object. A brief historical account of this problem tells it started out as an interest of the field of bubble cavitation in hydrodynamics and continued to attract a great deal of attention in modern research. Historically, the initial relevance was the problem concerning the damage caused by collapsing air bubbles in water. This process caused the erosion of screw propellers of ships and other naval structures. This is Lord Rayleigh's seminal contribution. Rayleigh began the field that produced a sequence of very interesting findings concerning the acoustic properties of bubbles. Initially, the theory he devised neglected both viscosity and surface tension (Rayleigh 1917). Later, in 1933, the physicist Marcel Minnaert became interested in knowing the origin of the noise that comes from the breaking of the waves at sea or, simply, the noise of running water. He reduced his deductive method to the elementary phenomena of a freely vibrating spherical bubble in water. Here, dissipative and surface tension were also neglected. In his findings he found the natural frequency of oscillation of the bubble's wall, since the oscillations of the gas trapped inside and the pressure of the liquid outside work analogously as a mass-spring system in a simple harmonic oscillator (Minnaert 1933, Leighton 1994, Ainslie and Leighton 2011). Without dissipation, bubbles can be long lasting in water and they vibrate freely at a frequency known as the Minnaert frequency. Incorporating surface tension and viscosity in Rayleigh's model leads to damping effects and temperature variations (Ainslie and Leighton 2011, Hickling and Plesset 1964). The interest in this field is still strong due to the fantastic results in bubble sonoluminescence where the energy focusing mechanism present in bubble oscillations and collapse, leads to light emission and temperatures of the order of the sun's surface (Putterman and Weninger 2000). Moreover, there are the significant findings on developments of contrast agents in biomedical research (Chomas et al. 2000) and new men made metamaterials as well (Bretagne et al. 2011, Leroy et al. 2015).

In revisiting the partial wave model applied to acoustic scattering one finds the work of Victor Anderson who showed that this formalism can be applied to the acoustic scattering of the bubble (Anderson 1950, Feuillade and Clay 1999). Although, the approach does not deal exclusively with a differential equation describing the dynamics of the radius of the bubble, it can also be generalized to consider damping effects. Along this same line, the modal approach, Hebert Überall identified promising research in the partial wave model and Minnaert's idea. He applied quantum mechanical theory of resonance scattering to the classical phenomenon of acoustic scattering from solid elastic targets (Flax et al. 1981). The application of resonance theory by Überall and co-workers opened up unexplored field. From hereon, it becomes clear that research in this area requires delving an interdisciplinary combination between hydrodynamics and resonance theory. It must be mentioned that the latter theme has also been thoroughly dealt with by Moyses Nussenzveig. Among the many works he authored, Nussenzveig gave physical interpretation to the scattering resonances of a spherical dielectric particle. Gustav Mie, in 1905, solved the problem of electromagnetic scattering by a dielectric sphere motivated by his interest to understand the colorful appearance of a gold colloids (Nussenzveig 1992, 1969). Within the intricate mathematical combinations of special functions in Mie's solution, Nussenzveig applied an analogy between resonances in potential scattering of quantum mechanics and electromagnetic scattering and reached physical interpretation where tunneling played a major role. This made accessible a better understanding of the main physical phenomena responsible for the long lived Mie resonances. Identifying a parallel between the works of Minnaert-Anderson-Uberall and Mie-Nussenzveig one can verify that the role of tunneling phenomena in the acoustic resonances of a spherical air filled bubble has not been explicitly considered before. Rayleigh's approach and success inspired many researchers in a continuous study of more elaborate models based on the differential equation that describes the dynamics

of the bubble's wall and damping through viscosity and surface tension. A comparison between the many different models and their principles can be found in the suggested references (Prosperetti 1984, Leighton 1994, Ainslie and Leighton 2011). Among all the existing models on this field, the authors have chosen the partial wave approach to study the proposed problem, since the important role of tunneling phenomenon on acoustic resonances can only be properly considered within this model.

Nowadays (Putterman and Weninger 2000, Chomas et al. 2000, Garbin et al. 2009, Thomas 2009, Pierre et al. 2014), the scattering of sound from spherical obstacles is an extremely important problem in many research areas such as, non-invasive medical diagnosis, and industry (Zinin and Allen III 2009, Strybulevych et al. 2012). In such problem, an incident acoustic wave, once scattered by an object, can excite mechanical vibrational modes of the scatterer (Landau and Lifshitz 1987). These vibrational modes are the source of secondary acoustic waves. These secondary waves are signatures of the self-sustained natural vibrations that can be excited through resonance mechanism. The acoustical spectrum detected can give many types of valuables informations about scattering objects. To this end, the development of complete theoretical models for scattering of single objects is necessary (Morse and Ingard 1968). The partial wave formalism is one of the methods for solving the problem. However, due to wave nature of this problem, we believe that a cautious analogy with similar electromagnetic and quantum mechanics problems can improve the understanding on this matter and in the next sections we will explore this possibility. From the acoustical point of view, this work revisits the previous fundamentals works of Anderson (Anderson 1950, Feuillade and Clay 1999). For this purpose, the excitation of normal modes of vibration of the air bubble in water is treated as a scattering problem, where viscosity is neglected both in air and water. In this model, a plane wave impinges on a spherical gas bubble in unbounded water (Morse and Ingard 1968, Anderson 1950, Feuillade and Clay 1999). In addition, the process of an oscillating force acting on the surface of the bubble, due to the difference in pressure fields, makes the bubble expand and collapse (Leighton 1994). The energy coupling mechanism between an internal pressure field and matter leads to the natural modes of vibration of the bubble surface. The signature of this natural vibration is unique as the sound emitted is solely due to a self-sustained mode of vibration. Experimental evidence is found on the detection of the frequency of microbubble vibration (Thomas et al. 2009). Applications of this property can be found in the fields of ultrasound contrast agents (Stride and Saffari 2003) and on the development and study of acoustic metamaterials (Leroy et al. 2015, Bretagne et al. 2011), where an array of bubbles, as well as liquid foams, can be used to block the transmission of sound. These metamaterials were used to completely block ultrasound transmission of some frequencies suggesting acoustic insulation (Thomas 2009, Pierre et al. 2014, Leroy et al. 2015).

In this manner, in this work we apply Nussenzveig's approach to the acoustic scattering by prescribing an effective potential to the bubble dynamics. This quantum mechanical technique can be applied in an analogy to acoustic scattering of a gas filled spherical cavity in a liquid. This analogy is a basic concept for understanding the nature of the bubble mechanical vibrations, since its analysis connects different phenomena linked by common properties or similar behavior. For instance, in this work we introduced the concept of "thin layer" in order to take into account the effects of high density water-air contrast in potential scattering, which resembles some features of the Woods-Saxon scattering potential in nuclear physics. Although quantum physics differs from classical physics in both formalism and fundamental concepts there are a large number of existing analogies between these fields. The present work calls into action two fundamental areas of physics: fluid mechanics and the scattering methods of quantum physics. The results show the possibil-

ity of attaining other regimes of the bubble surface vibration with much longer lifetimes than the Minnaert resonance. Here, wave tunneling plays a fundamental role.

The following sections discuss the problem of resonant acoustic scattering of a spherical bubble in more detail. To this end, the second section considers the partial wave series formalism applied to the scattering of an incident plane pressure wave by a spherical air bubble immersed in unbounded water. In the third section the condition for resonance regime is object of a deeper mathematical and physical inspection. In the fourth section, numerical procedures elaborated from the semiclassical methods are used to precise determination of the resonance positions and widths for the various acoustic oscillations regimes. Finally, the conclusion section summarizes the present theoretical findings and discusses their physical implications to relevant areas of acoustics.

2 - THEORY: PARTIAL WAVE EXPANSION FOR ACOUSTIC SCATTERING FROM AIR FILLED SPHERICAL BUBBLE IMMERSED IN LIQUID WATER

The problem of sound scattering in three dimensions is related to solutions of wave equations which governs the displacement potential u or pressure p (Olver 2014). The pressure function p can be taken as solution of the pressure wave equation in the spherical coordinate system (Anderson 1950, Feuillade and Clay 1999). In Fig. 1a the scattering configuration treated in this work is shown. A plane pressure wave is incident on the gaseous spherical bubble immersed in unbounded liquid water medium. Here, as a first approximation any viscosity effect is neglected and the inhomogeneous media is comprised of the inner gaseous spherical bubble immersed in an unbounded liquid medium, which is water (see Fig. 1a). In other words, for a source-less medium and in a given instant of time t the pressure function $p(\vec{r},t)$ can be given for any point $\vec{r}$ and it satisfies the following wave equation (Shew 1994, Feuillade and Clay 1999):

$$\widetilde{\rho}(\vec{r})\vec{\nabla}\cdot\Big[\frac{1}{\widetilde{\rho}(\vec{r})}\vec{\nabla}p(\vec{r},t)\Big]-\frac{1}{c^2(\vec{r})}\frac{\partial^2 p(\vec{r},t)}{\partial t^2}=0. \tag{1}$$

Here, it is assumed that the media is characterized by density $\widetilde{\rho}(\vec{r})$ and sound speed $c(\vec{r})$ functions respectively. Besides, due to the spherical symmetry of the scattering object it is suitable to solve Eq. 1 in spherical coordinate system (r,θ,ϕ). In addition, the incident plane wave oscillates harmonically with an angular frequency given by ω. So, for all space the pressure function should take the form,

$$p(\vec{r},t)\equiv p(r,\theta,\phi,\omega)e^{-i\omega t}. \tag{2}$$

Moreover, the inhomogeneity of the medium is properly described by sound speed and density contrasts, respectively represented by:

$$c(\vec{r})=c(r)=\begin{cases}c_1 & \text{for } 0\leq r<a,\\ c_2 & \text{for } r>a.\end{cases} \tag{3}$$

They are as follows: c_1 is the speed of sound within the bubble, the gaseous medium, c_2 is the speed of sound in water. Besides, the media densities are such that

$$\widetilde{\rho}(\vec{r})=\widetilde{\rho}(r)=\begin{cases}\rho_1 & \text{for } 0\leq r<a,\\ \rho_2 & \text{for } r>a.\end{cases} \tag{4}$$

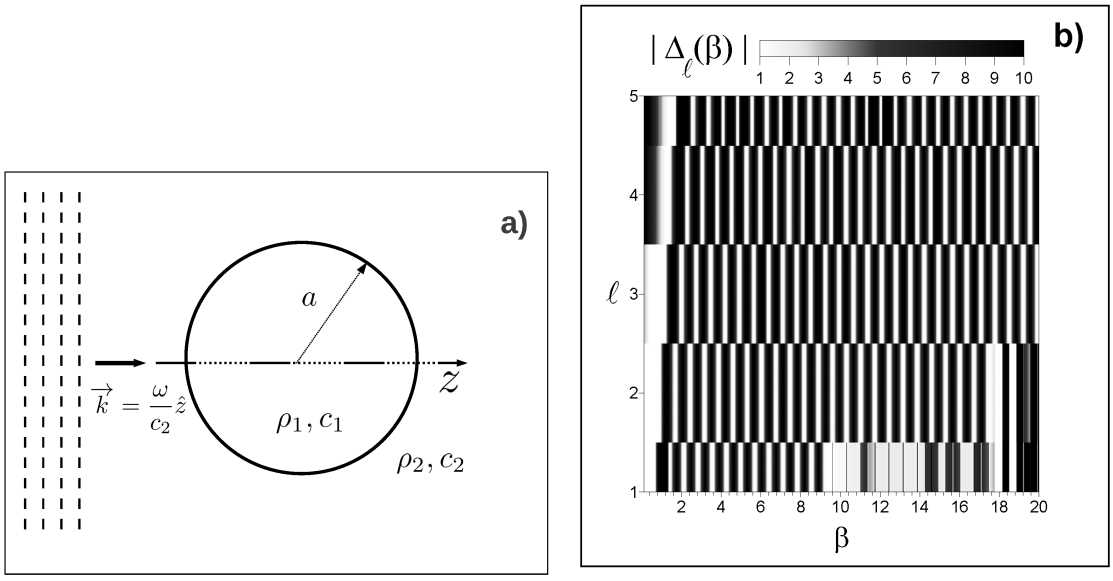

Figure 1 - The left panel (**a**) shows the scattering geometry, for an incident acoustic plane wave with related wave vector $\vec{k}$. The incident wave reaches a spherical gaseous bubble of radius $r = a$ surrounded by unbounded liquid water. Being the related sound velocity $c_1 = 340m/s$ and $c_2 = 1500m/s$ as well as the assumption of the densities values as $\rho_1 = 1.269kg/m^3$ and $\rho_2 = 999.972kg/m^3$ respectively. The right panel (**b**) shows for this scattering scenario, the strong oscillating behavior of the transcendental equation (see Eq. 13) $\Delta_\ell(\beta)$ in the plane $[\ell, \beta]$. In this gray scale color map, the white color is related to values of $|\Delta_\ell(\beta)| < 1$ and the black color as $|\Delta_\ell(\beta)| > 10$.

In this case, ρ_1 is the density of the gaseous medium and ρ_2 the density of the water. For the sake of simplicity, from hereon in, it is assumed that $\rho_2 > \rho_1$ and $c_2 > c_1$. In Anderson's work the partial wave expansion in spherical coordinates is developed for the spherical gas bubble (Anderson 1950, Feuillade and Clay 1999). The present work follows similar approach, such that the wave number in the two medium are $k_2 = \omega/c_2$ and $k_1 = \omega/c_1$ and for pedagogical reasons it is suitable employ the following notation, namely:

$$N \equiv \frac{c_2}{c_1} > 1. \tag{5}$$

and

$$\rho \equiv \frac{\rho_2}{\rho_1} > 1. \tag{6}$$

The ratio N is defined as the relative refractive index and ρ as the relative density respectively. Moreover, being a the radius of the bubble, it is suitable to define the dimensionless size parameters $\beta \equiv k_2 a$ and $\alpha \equiv k_1 a = N\beta$ related to wavelengths in outer (water) and inner (gaseous spherical bubble) regions respectively. Due to azimuthal symmetry, the pressure field in Eq. 2 can be expanded in the following partial wave series:

$$p(r, \theta, \omega) = \sum_{\ell=0}^{\infty} p_\ell(r, \theta, \omega). \tag{7}$$

Where the partial wave solution of the wave equation for pressure p_ℓ is obtained by applying the separation of variables method to Eq. 1 in the spherical coordinate system. The result can be written as the following product of functions (Anderson 1950, Feuillade and Clay 1999):

$$p_\ell(r,\theta,\omega) = R_\ell(r,\omega)P_\ell(\theta). \tag{8}$$

The function $R_\ell(r,\omega)$ represent the solutions of the differential spherical-Bessel equation and $P_\ell(\theta)$ represent the Legendre polynomials (Anderson 1950, Feuillade and Clay 1999). Hence, in the case of an incident plane wave of amplitude P_{inc}, the partial wave p_ℓ is explicitly given by:

$$p_\ell(r,\theta,\omega) = -P_{inc}i^\ell(2\ell+1)P_\ell(\theta) \times \begin{cases} 1 + E_\ell\, h_\ell^1(\beta r/a) & ; \quad a \le r < \infty \\ \\ D_\ell\, j_\ell(\alpha r/a) & ; \quad 0 \le r \le a. \end{cases} \tag{9}$$

The functions $j_\ell(x)$ and $h_\ell^1(x)$ are the spherical Bessel and spherical Hankel functions respectively. The coefficients E_ℓ and D_ℓ are obtained by applying the boundary conditions of continuity of the pressure and the radial particle velocity at the bubble's surface ($r = a$), namely (Anderson 1950, Feuillade and Clay 1999):

$$D_\ell = \frac{j_\ell'(\alpha)j_\ell(\beta) - ghj_\ell'(\beta)j_\ell(\alpha)}{j_\ell'(\alpha)h_\ell^1(\beta) - ghh_\ell'^1(\beta)j_\ell(\alpha)}, \tag{10}$$

$$E_\ell = gh\left[\frac{h_\ell'^1(\beta)j_\ell(\beta) - h_\ell'(\beta)j_\ell'(\beta)}{j_\ell'(\alpha)h_\ell^1(\beta) - ghh_\ell'^1(\beta)j_\ell(\alpha)}\right]. \tag{11}$$

Where the parameters $h = 1/N$, $g = 1/\rho$ as well as $j_\ell'(x)$ and $h_\ell'^1(x)$ are the first derivative, with respect to argument, of the spherical Bessel and spherical Hankel functions respectively (Anderson 1950, Feuillade and Clay 1999). Moreover, Bessel and Hankel functions are known to present oscillatory behavior. It is worth mentioning that there is a common denominator in Eqs. (10 and 11). Most importantly, for a certain discrete set of the parameters $\{\ell, \beta\}$ the denominator of these coefficients may assume very small values, therefore leading to extremely high peak amplitudes (Flax et al. 1981) in Eq. 10 and Eq. 11. The present study aims the search of the domain of parameters that produce maximum values of these coefficients (Flax et al. 1981). To this end, the denominator of the coefficients is isolated for a close inspection due to their important role in the discussions that follows. Simple algebraic manipulation leads to:

$$\frac{h_\ell'^1(\beta)}{h_\ell^1(\beta)} - \frac{\rho_2}{\rho_1}\frac{c_2}{c_1}\frac{j_\ell'(\alpha)}{j_\ell(\alpha)} = 0. \tag{12}$$

For the sake of compact representation the following notation is adopted (Nussenzveig 1969, 1992, Guimarães and Nussenzveig 1992):

$$\Delta_\ell(\beta) \equiv [1\beta] - \rho N[\alpha] = 0. \tag{13}$$

where

$$[1\beta] \equiv \frac{h_\ell'^1(\beta)}{h_\ell^1(\beta)}, \tag{14}$$

$$[\alpha] \equiv \frac{j_\ell'(\alpha)}{j_\ell(\alpha)}. \tag{15}$$

The transcendental equation $\Delta_\ell(\beta)$ in Eq. 13 can be solved in the $\beta-$complex plane with appropriate methods (Nussenzveig 1969, 1992, Guimarães and Nussenzveig 1992). In this plane, where $i \equiv \sqrt{-1}$, the solutions of this equation are generically expressed as:

$$\bar{\beta} = \beta - i\, b, \tag{16}$$

where β is the resonance position and b is the related resonance width (Nussenzveig 1969, 1992, Guimarães and Nussenzveig 1992). In general, the task of obtaining accurate solutions of Eq. 13 it is no longer trivial, since $\Delta_\ell(\beta)$ is a strong oscillating complex function (Nussenzveig 1969, 1992, Guimarães and Nussenzveig 1992). For more details, notice in Fig. 1b the complex behavior of the function $\Delta_\ell(\beta)$ in the plane $[\ell, \beta]$. In the next section a semiclassical theory is devised so as to obtain explicit formulas for accurate numerical calculations and physical interpretation to the solutions of Eq. 13.

3 - SEMICLASSICAL THEORY FOR ACOUSTIC RESONANT MODES OF A SPHERICAL AIR BUBBLE IN WATER

It follows from the wave equation in Eq. 1 and the partial wave analysis in Eq. 8, that any radial function $R_\ell(r, \omega)$ must satisfy the following differential equation:

$$\frac{1}{r}\left\{\frac{d^2}{dr^2}(rR_\ell)\right\} + \left\{\frac{\omega^2}{c^2(r)} - \frac{\ell(\ell+1)}{r^2}\right\} R_\ell - \frac{1}{\widetilde{\rho}(r)}\frac{d\widetilde{\rho}}{dr}\frac{dR_\ell}{dr} = 0 \tag{17}$$

As seen from Eq. 4 the value of the density $\widetilde{\rho}$ is not well defined at $r = a$. Therefore, the density function should behave more like a distribution function. In order to estimate the physical implications of the discontinuity of $\widetilde{\rho}$ to the sound propagation within the interior region of the bubble, it is assumed that the density $\widetilde{\rho}$ is represented by a distribution function. In other words, we assume here that this function must be continuous and differentiable on the whole space. More specifically, it is assumed that around the boundary spherical interface $r = a$ there exists a *very thin layer* of transition between the density values of the air as well as of the water. This means that the density $\widetilde{\rho}(r)$ must continuously vary from the air to water density values. Explicitly, the physical features of the transition layer are represented by $\widetilde{\rho}(r)$ given that:

$$\widetilde{\rho}(r) \approx \sqrt{\rho_2\rho_1}\left\{\frac{\rho_2}{\rho_1}\right\}^{\frac{1}{2}\left[\tanh\frac{2(r-a)}{\delta a}\right]}; 0 \le r < \infty. \tag{18}$$

Where the positive parameter $\delta a \ll a$ is the width of the *thin transition layer*. This width is a real physical quantity corresponding to a thin spherical shell. It should behave as a result of a mixture of air and the accumulated water vapor on regions close to the boundary of the mathematical bubble surface at $r = a$. The function in Eq. 18 is shown in Fig. 2. In this figure the *thin transition layer* δa is sketched exaggeratedly. It is possible to note the $\widetilde{\rho}$ density transition behavior between air and water. More specifically, when $r = a$ in Eq. 18 the function $\widetilde{\rho}$ results in the geometric mean $\sqrt{\rho_1\rho_2}$ and as $\delta a \to 0$, Eq. 18 tends to piecewise Eq. 4 as well. Besides, based on distribution theory and assuming regions not so close to geometrical interface $r = a$, the following relation can be considered,

$$\frac{dR_\ell}{dr}\left(\frac{1}{\widetilde{\rho}}\frac{d\widetilde{\rho}}{dr}\right) \to \left\{-\frac{d^2\ln\widetilde{\rho}}{dr^2}R_\ell\right\}. \tag{19}$$

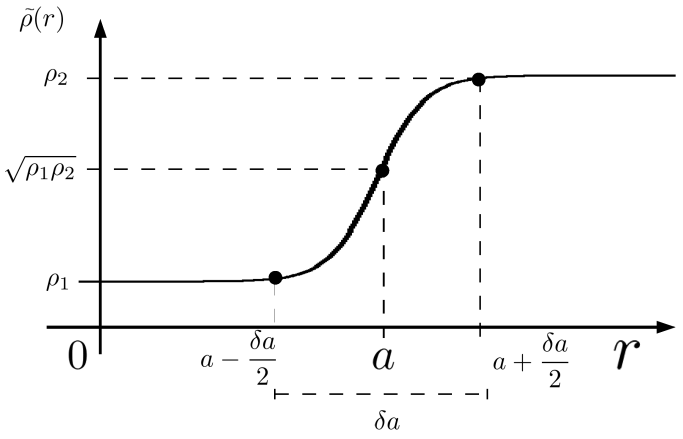

Figure 2 - Sketches a model (see Eq. 18) to the behavior of the density $\widetilde{\rho}$ around the bubble interface between water and air, where it is assumed that a *thin layer* of width δa separates the two media. The inner medium (the air) has density ρ_1 and ρ_2 is the density of the outer medium (water).

With this in mind, it is possible to rewrite the radial equation in Eq. 17 suitably in an expression which resembles a Schrödinger-like equation of the form (Guimarães and Nussenzveig 1992, Schiff 1968, Griffths 2005),

$$-\frac{1}{r}\frac{d^2}{dr^2}(rR_\ell)+U_{eff}(r)R_\ell=\left(\frac{\omega}{c_2}\right)^2R_\ell. \tag{20}$$

Henceforth, the Quantum Mechanics formalism can be introduced and applied to make the corresponding interpretations. In other words, it is possible to solve the differential equation in Eq. 20 and obtain solutions in an analogy with potential scattering in Quantum Mechanics (Nussenzveig and Wiscombe 1987, Guimarães and Nussenzveig 1992, Griffths 2005). In this framework (in units of "$\hbar\equiv 1$ " and "$2m\equiv 1$"), the sound plane wave is interpreted as an incident "particle" with "positive energy $(\omega/c_2)^2$ " subjected to an acoustical scattering effective potential U_{eff} given as,

$$U_{eff}(r)=\frac{\ell(\ell+1)}{r^2}-\left(\frac{\omega}{c_2}\right)^2\Big[N^2-1\Big]-\frac{d^2}{dr^2}[\ln\widetilde{\rho}]. \tag{21}$$

In Fig. 3 the graphical representation of the function U_{eff} in Eq. 21 is shown. Notice that the effective potential U_{eff} is composed by three independent terms, namely: The "repulsive centrifugal barrier"$\Delta U_\ell(r)$,

$$\Delta U_\ell(r)\equiv\frac{\ell(\ell+1)}{r^2}\ , \tag{22}$$

and two "attractive potential wells". These last "potential wells"are related to variations in values of sound speed as well as abrupt density changes in bubble air-water interface respectively. In other words, the ef-

fective potential U_{eff} has contributions due to the "refractive index well"ΔU_N and the "contrast density well"ΔU_ρ. Which are given by respectively:

$$\Delta U_N(r) \equiv -\Big(\frac{\omega}{c_2}\Big)^2\Big[N^2-1\Big], \tag{23}$$

and

$$\Delta U_\rho(r) \equiv -\frac{d^2}{dr^2}[\ln\widetilde{\rho}]. \tag{24}$$

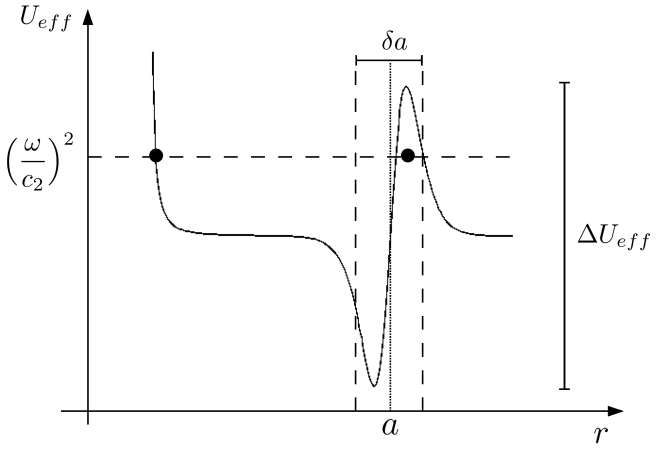

Figure 3 - Sketches the behavior of the effective potential U_{eff} as a function of the radial coordinate r. The incident sound wave is related to the incident particle of "energy" $(\omega/c_2)^2$. The "potential barrier" ΔU_{eff} (see Eq. 25) is also shown.

According to the analogy proposed, the nearly "bound-states" of sound are, in fact, the ones related to the acoustical resonances that are nearly trapped inside the bubble. The term "quasi bound state" (QBS) of sound is here employed to designate these special modes of vibration that resemble atomic bound states of limited lifetime. The word "quasi" is appropriate because of the radiating mechanism played by tunneling effect that lead to limited lifetime. Tunneling is a natural wave phenomena related to propagation of evanescent waves, occurring in quantum as well as in classical frameworks (Guimarães and Nussenzveig 1992). The QBS resonance like has a determined time for its existence in the inner medium. This "mean lifetime" is related to b the widths of the resonance (Guimarães and Nussenzveig 1992), which is strongly influenced by behavior of the "energy barrier" ΔU_{eff} given here as,

$$\Delta U_{eff} = \Big(\frac{\omega}{c_2}\Big)^2[N^2-1] + \frac{16\sqrt{3}}{9}\frac{\ln\big[\rho\big]}{\delta a^2}. \tag{25}$$

Notice that ΔU_{eff} is a function of N, ρ and δa, but it does not explicitly depend on multipole order ℓ (see Fig. 3). Besides, it should be recalled that a narrow resonance width b implies in a longer lifetime of the resonant stationary wave inside the bubble, since it is expected that the resonance widths b decrease as the

height of ΔU_{eff} increases (Guimarães and Nussenzveig 1992, Schiff 1968, Griffths 2005). Equation (25) suggests that this mechanism might occur when the relative refractive index N and relative density ρ are considerably high as well as the boundary surface layer depth δa is very thin. In fact, in the case of the spherical gaseous bubble in water, due to high contrast between sound speeds and densities media $N \gg 1$ and $\rho \gg 1$ is a phenomenological reality. Besides, the mixture of air with water vapor accumulated around the boundary $r = a$ gives rise to a very thin layer medium where $\delta a \ll a$.

Within this context, it is feasible to assume the thin layer approximation in Eq. 18 presented above, where the density transition region becomes a continuous function of the distance r. In the following subsections, this approximation is used to obtain accurate resonance estimations and overview all the inherent implications of the former evidences. In addition, it is important to note that the scattering potential in Eq. 21 permits the application of semiclassical methods, such as the JWBK theory (Guimarães and Nussenzveig 1992). This will lead to important mathematical relations that quantify the relevant physical parameters related to present resonant bubble scattering problem.

Semiclassical Analysis for Bubble Acoustic Resonant Scattering

Within the analogy commonly found relating classical scattering and quantum scattering (Nussenzveig 1969, 1992), a semiclassical analysis is applied so as to evidence the important physical aspects of the problem of the scattering of sound by an air bubble in water. Scattering problems often deal with incident particles, classical or quantum, which interact with targets with some internal structure. In this context, it is straightforward to introduce the conceptual meaning of some scattering parameters.

Firstly, let us consider the situation where the penetrable scattering target is positioned at large distance d from the incident particle (see Figs. 4a and b). In addition, we assume that for distance $d >> a$ the interaction of this idealized particle with the short range central force field potential U_{eff} (Eq. 21) is negligible. With this idea in mind, the concept of the impact parameter I can be introduced and its relation with the angular momentum "quantum number" ℓ can be sought for. In far field region $d >> a$ and following de Broglie and Planck (Schiff 1968), the semiclassical linear momentum of the incident "free particle" has magnitude $\hbar k$ (with $k \equiv \omega/c_2 = k_2$) where $\hbar$ is Planck's constant reduced. Moreover, due to symmetry of this problem, it is possible to apply the Sommerfeld's quantization rule (Schiff 1968) to the conservation of total angular momentum and to establish the relation between ℓ and impact parameter I, namely:

$$\hbar k I = \hbar\sqrt{\ell\,(\ell+1)} \approx \hbar(\ell + 1/2), \tag{26}$$

Where within the semiclassical framework the Langer modification $\ell(\ell+1) \to (\ell+1/2)^2$ was introduced (Schiff 1968). So it follows from Eq. 26 that,

$$I \to I_\ell = \frac{(\ell + 1/2)}{k}. \tag{27}$$

where I_ℓ is the related partial wave impact parameter. The geometrical meaning of I_ℓ can be readily visualized in Fig. 4a and Fig. 4b. In the first case (see Fig. 4a), it is verified that

$$\frac{(\ell + 1/2)}{k} = I_\ell > a, \tag{28}$$

hence

$$(\ell + 1/2) > \beta. \tag{29}$$

In similar manner, for the second case (see Fig. 4b), it is verified that

$$(\ell + 1/2) < \beta. \tag{30}$$

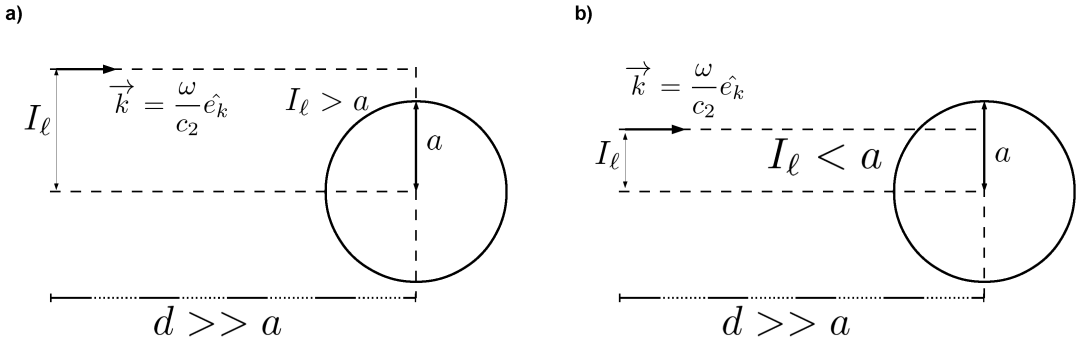

Figure 4 - Shows the scattering geometry in two distinct situations. In (**a**) is the case where the magnitude of the impact parameter (I_ℓ) is $I_\ell > a$ and in (**b**) is $I_\ell < a$.

On the other hand, in optics, when the refraction index of a spherical dielectric particle is $N > 1$, it follows from the analogy between optics and other types of waves that the region with high intensity (caustics) is limited between aplanatic spheres exterior and interior to the scattering target (Born and Wolf 1975). Here, the same interpretation is made to the acoustical scattering potential U_{eff} in Eq. 21, where now the radii of these regions are given respectively as,

$$R_{ext} \equiv Na\ , \tag{31}$$

and

$$R_{int} \equiv \frac{a}{N}\ . \tag{32}$$

So, from Fig. 4a and Fig. 4b and Eq. 31 it can be seen that the partial impact parameters I_ℓ which is associated with highly intense sound fields must satisfy the following geometrical criteria:

$$d >> R_{ext} >> I_\ell, \tag{33}$$

in other words,

$$d >> Na >> \frac{\ell + 1/2}{k}\ . \tag{34}$$

This means that Eqs. (29, 30 and 34), suggest that there are two distinct types of scattering which permit the build up of very intense sound fields. In the first case it follows from Eqs. (29 and 34) that the size parameters should satisfy the following inequality:

$$\beta < (\ell + 1/2) < \alpha\ . \tag{35}$$

The other case, which follows from Eqs. (30 and 34), results in another inequality:

$$(\ell + 1/2) < \beta < \alpha\ . \tag{36}$$

The criteria for resonance phenomenon is now examined. Firstly, the inequality in Eq. 35 is carefully examined and secondly, the condition expressed in Eq. 36 is then dealt with.

The Acoustic "Quasi-Bound States" Resonant Modes of the Bubble

Earlier in this work it was put forward that the poles of the coefficients in Eqs. (10 and 11) of the partial wave expansion are solutions of the complex transcendental equation in Eq. 13. From the fact that in this situation $\alpha > (\ell + 1/2)$, the Debye approximation (Debye 1909, Watson 1944, Abramowitz and Stegun 1972) for the Bessel functions gives us the following result,

$$[\alpha] \approx -\frac{\sqrt{\alpha^2 - (\ell+1/2)^2}}{\alpha} \tan[\phi(\alpha, \ell+1/2) - \frac{\pi}{4}] \,, \tag{37}$$

where $\phi(\alpha, \ell + 1/2)$ is given from the Bohr-Sommerfeld integral (Schiff 1968), namely:

$$\phi(\alpha, \ell+1/2) \equiv \int_{r_1}^{a} dr \sqrt{k^2 - U_{eff}} \,. \tag{38}$$

Where the internal turning point $r_1 < a$ in the interior of the bubble (see Fig. 5a) should satisfy $U_{eff}(r_1) = k^2$ and it is given as,

$$r_1 = \frac{\ell + 1/2}{kN} = \frac{I_\ell}{N} \,. \tag{39}$$

Besides, in present problem we have $R_{int} < r_1$ (see Eq. 32, Figs. 5a and 6a), consequently the total internal reflection condition is always fulfilled, namely:

$$\frac{a}{N} < r_1 \Rightarrow sin\,(\theta_c) = \frac{1}{N} < \frac{r_1}{a} = sin\,(\theta_R) \,. \tag{40}$$

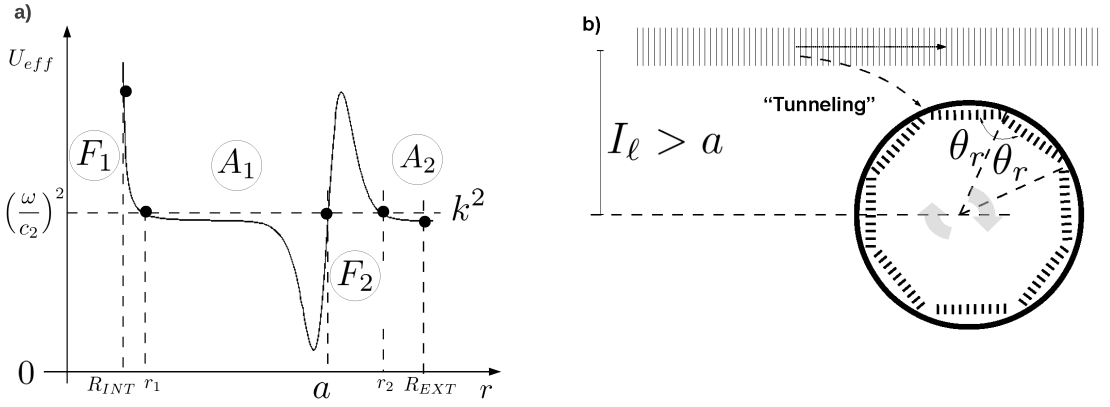

Figure 5 - In (**a**), for a given incident "particle" with positive energy k^2 ($k \equiv \omega/c_2$) is shown the "Energy budget" mechanism associated with the "excitation" of resonant "Quasi-Bound States"(QBS). Notice that $r_2 = I_\ell = (\ell + 1/2)/k$ and $r_1 = I_\ell/N$. In (**a**), the classically allowed regions A_1 and A_2 correspond to propagating waves, whereas the classically forbidden regions F_1 and F_2 are related to the evanescent waves. Figure (**b**) shows the equivalent ray-trajectory picture related to these resonances.

Moreover, considering the domain of the thin boundary layer approximation $\delta a \to 0$ the integral Eq. 38 gives the following approximation:

$$\phi(\alpha, \ell+1/2) \approx \sqrt{\alpha^2 - (\ell+1/2)^2} - (\ell+1/2) \arctan\left[\frac{\sqrt{\alpha^2 - (\ell+1/2)^2}}{(\ell+1/2)}\right] \,. \tag{41}$$

On the other hand, in the case of the external turning point $r_2 > a$, being r_2 solution of $U_{eff}(r_2) = k^2$, it can also be observed that Eq. 35 can be rewritten as:

$$a < \frac{(\ell + 1/2)}{k} \equiv r_2 = I_\ell < R_{ext} \, . \tag{42}$$

This situation can be readily be seen graphically in Fig. 5a. This figure shows the quasi-bound states (Guimarães and Nussenzveig 1992) or a metastable state (Schiff 1968) which can occur when the effective potential U_{eff} allows the existence of three turning points, r_1, a and r_2. In this particular case there can be found, in the scattering dynamics, a stationary wave (Guimarães and Nussenzveig 1992, Schiff 1968) in the region usually called classically allowed A1 ($r_1 \leq r \leq a$), and these waves can be coupled to the continuum behaving like progressively propagating waves in the other classically allowed region A2 ($r > r_2$). The ray picture trajectory can be associated with this scattering geometry, where in Fig. 5b it is seen an incident acoustic plane wave with an associated value for the impact parameter I_ℓ that is considerably greater than the sphere radius a. In other words, the incident particle which in realistic terms is an acoustic plane wave, tunnels the barrier U_{eff} (Eq. 21) and is kept within the bubble through orbiting the inner boundary by nearly-total internal reflections. In addition, in the present ray picture (see Eq. 40, Figs. 5 and 6), for the case where the incident wave tunnels into the bubble, the internal incidence angle θ_R is above the critical value $\theta_c = arcsin(1/N)$. The tunneled wave gets successively internally reflected and excites modes with high lifetime values (Guimarães and Nussenzveig 1992). In these cases, inside the other two classically forbidden regions F1 ($0 < r < r_1$) and F2 ($a < r < r_2$) the waves become evanescent. Moreover, in this semiclassical regime, $[1\beta]$ can be expressed in the Debye approximation (Debye 1909, Watson 1944, Abramowitz and Stegun 1972) as:

$$[1\beta] \approx -\frac{\sqrt{(\ell + 1/2)^2 - \beta^2}}{\beta}[1 - ie^{-2\psi}]. \tag{43}$$

Where $\psi(\beta, \ell{+}1/2)$ is the Gamow integral (Schiff 1968, Griffths 2005) related to tunneling in the classically forbidden region F2 and it is given by:

$$\psi(\beta, \ell + 1/2) \equiv \int_a^{r_2} dr \sqrt{U_{eff} - k^2}. \tag{44}$$

Besides, taking again the thin boundary layer limit $\delta a \to 0$, this integral can be approximated by:

$$\psi(\beta, \ell + 1/2) \approx (\ell + 1/2) \ln \Big[\frac{(\ell + 1/2) + \sqrt{(\ell + 1/2)^2 - \beta^2}}{\beta}\Big] - \sqrt{(\ell + 1/2)^2 - \beta^2} \, . \tag{45}$$

Together with Fig. 4a and Fig. 5a it can be seen that the underpinning for the physical mechanism of the quasi-bound states resonances in the interior of the bubble is solely related to tunneling (Guimarães and Nussenzveig 1992). So, in these semiclassical approximations the complex solutions $\bar{\beta} = \beta - ib$ of Eq. 13 must satisfy the following transcendental equation:

$$\tan\Big[\phi(N\bar{\beta}, \ell + 1/2) - \pi/4\Big] = \frac{1}{\rho}\sqrt{\frac{(\ell + 1/2)^2 - \bar{\beta}^2}{(N\bar{\beta})^2 - (\ell + 1/2)^2}}\Big[1 - ie^{-2\psi(\bar{\beta}, \ell + 1/2)}\Big] \, . \tag{46}$$

This equation is here solved assuming the approximation of the high density contrast between the media ($\rho >> 1$) and also in the regime of very narrow resonances where,

$$0 < b \ll \beta \, . \tag{47}$$

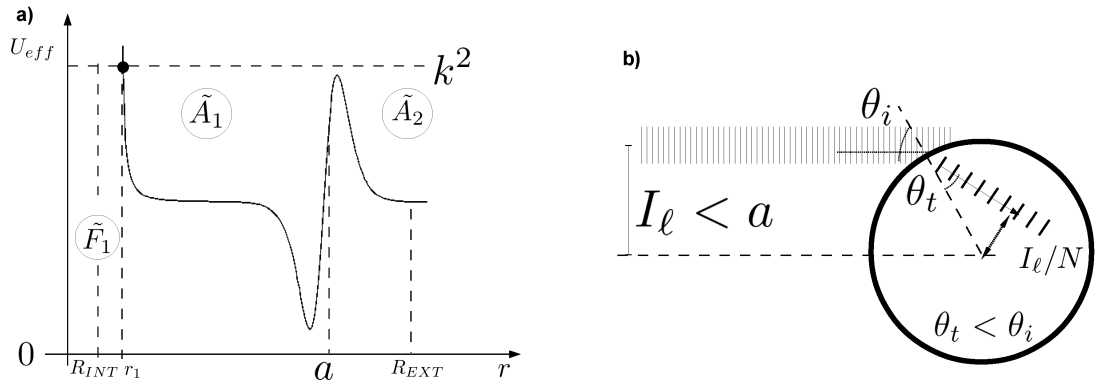

Figure 6 - In (**a**): Similar to Fig. 5, shows the "Energy budget" mechanism associated with the "excitation" of the Transmission Resonances (TR) associated to one classically forbidden region $\tilde{F_1}$ and two classically allowed regions $\tilde{A_1}$ and $\tilde{A_2}$ respectively. In (**b**) the figure shows the equivalent ray trajectory picture, where the incident acoustic plane wave, for a given impact parameter I_ℓ, makes a direct collision with the spherical surface of the bubble. A fraction of the incident beam is refracted at angle θ_t which is smaller than the incidence angle θ_i.

Taking the above facts in account, Eq. 46 is now given by the following set of coupled equations,

$$\phi(N\beta, \ell + 1/2) \approx (n + 1/4)\pi + \frac{1}{\rho}\Big[\sqrt{\frac{(\ell+1/2)^2 - \beta^2}{(N\beta)^2 - (\ell+1/2)^2}}\Big] \tag{48}$$

and

$$b \approx \frac{\beta}{\rho}\frac{\sqrt{(\ell+1/2)^2 - \beta^2}}{[(N\beta)^2 - (\ell+1/2)^2]} e^{-2\psi(\beta, \ell+1/2)} \, . \tag{49}$$

Equation (48) shows that for a given multipole ℓ, the resonant size parameters β assume discrete values as $\beta \to \beta_{\ell,n}$, where the mode index or order are integers such that $n = 0, 1, ...n_{max}$, being $n_{max} + 1$ the maximal number of QBS resonances that are allowed to exist related to multipole ℓ. Notice that in Eq. 49 that the resonance width b is proportional to the penetration factor $e^{-2\psi}$, that in Quantum Mechanics framework (Nussenzveig 1969, Guimarães and Nussenzveig 1992), it is analogous to the probability to find the particle into the centrifugal barrier ΔU_ℓ(22). In addition, within the approximation of $\beta_{\ell,n} << (\ell + 1/2)$ it follows from Eq. 48 that a rough estimation for $\beta_{\ell,n}$ is given by:

$$\beta_{\ell,n} \approx \frac{\pi}{N}(\ell/2 + n) + \frac{(\ell+1/2)}{\rho\pi N^2(n - 1/4)}, \tag{50}$$

when $\beta_{\ell,n} \to (\ell + 1/2)$ it can be estimated from above Eq. 50 that n_{max} must satisfy,

$$n_{max} \approx int[\ell(\frac{N}{\pi} + \frac{8}{\pi^3\rho} - \frac{1}{2}) + \frac{2}{N\rho\pi^2}] \, , \tag{51}$$

where $int[a]$ is the integer part of a.

In order to clarify the meaningful results, a comparison between some scattering processes time scales is now considered. For instance, for a given resonant multipole with order ℓ and applying Heisenberg's

uncertainty principle (Schiff 1968), it is possible to estimate τ_ℓ the related mean lifetime as (Guimarães and Nussenzveig 1992),

$$\tau_\ell \approx \left(\frac{2\pi a}{c_1}\right)\frac{1}{Nb_\ell}\,. \tag{52}$$

Since the sound velocity inside the bubble is c_1, the wave spends a time interval around $(2\pi a/c_1)$ to give a complete turn in regions near the surface $r = a$. In addition, in this semiclassical regime of narrow resonance (Guimarães and Nussenzveig 1992) shown in Eq. 47, the internal bubble surface transmission coefficient behaves as Nb_ℓ, so the internal wave total number of turns can be asymptotically estimated as $1/(Nb_\ell)$. Furthermore, τ_ℓ can be interpreted as the time scale in which the resonant acoustic energy stays trapped by internal multi-reflections inside the bubble. Moreover, the time related to bubble surface oscillations (Devaud et al. 2008) is the Minnaert's (Minnaert 1933) period T_M, that is given by:

$$T_M = \frac{2\pi}{\omega_M}, \tag{53}$$

with ω_M as Minnaert's angular frequency (Minnaert 1933, Devaud et al. 2008, Ainslie and Leighton 2011) written as,

$$\omega_M = \sqrt{\frac{3c_1^2\rho_1}{a^2\rho_2}}\,. \tag{54}$$

So, an inspection of τ_ℓ for a QBS resonance phenomena permits a comparison between the period of the incident wave $T \equiv 2\pi/\omega$, T_M and τ_ℓ. It follows from Eqs. (49 and 52) in the limit where $\beta_{\ell,n} << (\ell+1/2)$ that,

$$\tau_\ell \approx \frac{3T_M^2}{T}e^{2\ell ln(\ell+1/2)} \gg T_M. \tag{55}$$

It is verified that Minnaert's period T_M arises here as a natural time scale, since it is the shortest period of time associated to an acoustic resonance frequency, establishing a natural lower limit to such time scale. The expression in Eq. 55 tells us that the acoustic resonant energy stays confined in the interior of the bubble even after a great number of cycles of the bubble surface oscillations. Showing that the bubble in a QBS resonance regime is a robust resonant acoustic cavity with an extremely high quality factor Q_ℓ given by,

$$Q_\ell \equiv \beta_\ell/b_\ell \approx \tau_\ell/T\,. \tag{56}$$

In other words, the bubble is a resonant cavity that supports mechanical variations of its surface without strong attenuation of the related ℓ-th acoustic multipolar resonant QBS mode (Flax et al. 1981), even in the regime of small values of the multipole ℓ. In addition, when compared to other resonant cavities this special acoustical bubble feature is not found in others well established high–Q resonant cavities such as Fabry-Perot like electromagnetic superconducting (Blais et al. 2004) or, even still, in Lasing microdroplets associated to Mie resonances (Alexandr et al. 2012).

The Acoustic "Transmission Resonances" Modes of the Bubble

Let us discuss another possible resonance behavior case, the one shown in Fig. 4b, where the impact parameter $I_\ell = (\ell+1/2)/k$ is smaller than the radius a of the spherical bubble. In this situation the scattering energy budget can be understood in Fig. 6a with an associated ray trajectory picture given in Fig. 6b. The total internal reflection criteria is satisfied either (see Eq. 40), but the scattering dynamics for this new configuration

is noticeably distinct from the previous case. Now there are only evanescent waves in a classically forbidden region (see Fig. 6a), named $\tilde{F}_1$ ($0 < r < r_1$), while in the classically allowed regions $\tilde{A}_1$ ($r_1 \leq r < a$) and $\tilde{A}_2$ ($r \geq a$) there are propagating waves. More specifically, in this particular case, the barrier ΔU_{eff}(25) is "almost transparent" to incident wave and by total internal reflection it can be trapped into the bubble. Fig. 6b shows this situation. A ray picture illustrates how the incident acoustic wave impinges the spherical surface of the bubble, and by refraction, is transmitted to the internal medium. In other words, for a given multipole ℓ, Figs. (6a and 6b) show in this case that it is possible excite an acoustic resonant mode that can undergo yet several internal reflections before decaying in a lifetime which is smaller than the corresponding QBS resonances.

For this new configuration, the physical mechanism that can generate highly intense acoustic fields in the interior of the bubble and in its surroundings is the constructive wave interference, that in quantum mechanic picture is related to the Transmission Resonance (TR), this last being very similar to the Ramsauer-Townsend effect in atomic physics (Schiff 1968, Griffths 2005). In order to investigate this subject in more details we adopt the semiclassical ideas again. So, for $\beta > (\ell + 1/2)$ Debye's approximation (Debye 1909, Watson 1944, Abramowitz and Stegun 1972) applied to Eq. 13 yields:

$$\tan[\phi(N\beta, \ell + 1/2) - \pi/4] \approx \frac{-i}{\rho}\sqrt{\frac{\beta^2 - (\ell + 1/2)^2}{(N\beta)^2 - (\ell + 1/2)^2}}\,. \tag{57}$$

Again, applying the sharp resonances approximation $\bar{\beta} = \beta - ib$ ($0 < b \ll \beta$), in Eq. 57, we obtain that:

$$\phi(N\beta_{\ell,n}, \ell + 1/2) \approx (n + 1/4)\pi,\ n > n_{max} \tag{58}$$

and

$$b_{\ell,n} \approx \frac{\beta_{\ell,n}}{\rho}\frac{\sqrt{\beta_{\ell,n}^2 - (\ell + 1/2)^2}}{\left[(N\beta_{\ell,n})^2 - (\ell + 1/2)^2\right]}, \tag{59}$$

which can be simplified to

$$b_{\ell,n} \approx b_{mx}\frac{\sqrt{1 - \left(\frac{\ell+1/2}{\beta_{\ell,n}}\right)^2}}{\left[1 - \left(\frac{\ell+1/2}{N\beta_{\ell,n}}\right)^2\right]}, \tag{60}$$

where for this particular case of transmission resonances,

$$b_{mx} \equiv 1/(\rho N^2) \tag{61}$$

is the maximum asymptotic value that resonance widths $b_{\ell,n}$(60) can attain. Notice that the value of b_{mx} in Eq. 61 depends only the relative refractive index N and density ρ. In addition, b_{mx} is a decreasing function of N and ρ. Moreover, in the high contrast limit where $\rho \gg 1$, Eq. 58 gives an explicit rough estimate to value of the resonance position $\beta_{\ell,n}$ which is

$$\beta_{\ell,n} \approx \frac{\pi}{N}(\ell/2 + n),\ n > n_{max}. \tag{62}$$

In this asymptotic limit of $\rho \gg 1$, the transmission resonance $\beta_{\ell,n}$ in Eq. 62 doesn't explicitly depend on the relative density ρ. Besides, analyzing the spacing between resonances, Eq. 62 shows that these transmission resonances lead to small resonant shifts such as,

$$\beta_{\ell+2\Delta n,n} \approx \beta_{\ell,n+\Delta n}\,. \tag{63}$$

In other words, in the partial wave series (Eq. 7) for the acoustic pressures fields, in the context of the transmission resonances, the many multipoles give rise to resonance position values which are extremely close, hereon in designated as "Quasi-Degenerate States" (QDS), in correspondence to the analogous condition in Quantum Mechanics (Schiff 1968, Griffths 2005). As an example, taking $\Delta n = \pm 1$ in Eq. 62 the result $\beta_{\ell\pm 2,n} \approx \beta_{\ell,n\pm 1}$ is obtained. So, the resonant multipoles of consecutive order and defined parity (even or odd) have similar values of the Transmission Resonance positions. In addition, in this TR regime the related resonance widths can be also very close to the constant asymptotic value b_{mx} which is analogous to similar QDS with "broken symmetry" problems in Quantum Mechanics (Schiff 1968). In this particular situation, it is important to note that the incident acoustic energy is partitioned between these Quasi-Degenerated Transmission Resonance modes.

On the other hand, it follows from Eqs. (60 and 52) that it is possible to verify that the mean lifetime τ_ℓ related to the ℓ–th multipolar transmission resonances can be estimated to be,

$$\tau_\ell \approx 3\frac{T_M^2}{T} > 3T_M > T_M. \tag{64}$$

Notice that in the above geometrical acoustic asymptotic regime, τ_ℓ does not depend on the multipole order ℓ. Moreover, the values of $\tau_\ell \approx O(T_M)$ can be reached when one takes the solutions of Eq. 13 in the geometrical acoustic limit, where the resonant bubble in ray picture resembles a Fabry-Perot optical cavity (Devaud et al. 2008). In addition, Eqs. (64 and 63) tell us that after many cycles of surface oscillation, the bubble can yet retain a considerable quantity of energy in its interior. This is due to the excitation of some degenerates modes under transmission resonances regime, including the ones associated to multipoles of lowest orders (Gaunaurd et al. 1979).

Finally, it is necessary to discuss the Minnaert resonance phenomenon based on present analogy between quantum mechanics and acoustic. First of all, it is important to comment the very low frequency Minnaert resonance. This occurs as a monopole mode (with $\ell = 0$) and it leads to a resonance excited inside the bubble (Gaunaurd et al. 1979). In this particular situation and in the present picture of Transmission Resonances with $\ell = 0$, it is possible to rewrite the inequality in Eq. 36 as:

$$0 \lesssim \beta < \alpha. \tag{65}$$

Thus, it is a special case where the analogy with the Ramsauer-Townsend effect is completely fulfilled [see Schiff's book (Schiff 1968), p. 123-124]. In other words, this transmission resonance is an internal bubble stationary *s-wave* like, an omnidirectional resonant monopole with $\ell = 0$, where the related size parameter β should satisfies the transcendental equation in Eq. 13. In this special case, the transcendental equation can be explicitly written as:

$$\tan(N\,\beta) = \frac{\rho\, N\,\beta}{i\beta - 1 + \rho}. \tag{66}$$

Taking the limits of high density contrast ($\rho \gg 1$) and very low frequency ($\beta \ll 1$), Eq. 66 for $\beta \to \beta_m$ can be approximated by:

$$\frac{1}{3}{\beta_m}^2 N^3 + \frac{{\beta_m}^2 N^3 - N}{\rho} + i\,\frac{\beta_m\, N}{\rho} \approx m\pi, \text{with } \; m = 0, 1, ... \tag{67}$$

The above Eq. 67 shows that the resonance shift $\Delta\beta_m \equiv \beta_{m+1} - \beta_m$ can be estimated by the following expression:

$$\beta_{m+1} \approx \beta_m + \frac{3\pi}{2\beta_m N^3}\left(1 - \frac{3}{\rho}\right) \tag{68}$$

This recurrence equation in Eq. 68 suggests that the value of resonance position increases as the order m increases and for $N \to \infty$, these kind of TR resonant modes could be quasi-degenerated either as well. In addition, Eq. 68 shows that it is possible to estimate the value of high order resonance position β_{m+1} using the value of β_m. Thus, it is initially suitable to solve the complex Eq. 67 for fundamental mode $m = 0$. This task can be performed in the limit of sharp resonances ($\beta_m \to \beta_m - ib_m$ with $b_m \ll \beta_m$), which results in the following expressions respectively:

$$\beta_0 \to \beta_M = \frac{\sqrt{3}}{N\sqrt{\rho}} \equiv a\frac{\omega_M}{c_2} \tag{69}$$

and

$$b_0 \to b_M = \frac{3}{2}\frac{1}{N^2\rho} = \frac{3}{2}\, b_{\max} \tag{70}$$

Where the formulae for Minnaert's angular frequency ω_M and resonance width b_{mx} are given by Eqs. (54 and 61) respectively. Therefore, the *Minnaert resonances family* which are the complex solutions of transcendental equation(66) can behave as quasi-degenerated transmission resonances either. More specifically, the expressions in Eqs. (68, 69 and 70) suggest that the fundamental mode $m = 0$ related to usual acoustic *Minnaert resonances is very similar to Ramsauer-Townsend resonance* in nuclear or atomic physics (Schiff 1968) and it is the *broadest bubble transmission resonances*, consequently its related lifetime τ_M is the shortest and it can be estimated as,

$$\tau_M \approx 2T_M\ . \tag{71}$$

Thus, in this case of Minnaert like resonances the acoustic energy is sustained within the bubble approximately only during two cycles of bubble surface oscillations.

4 - RESULTS

This section discusses accurate numerical calculations designed to solve Eq. 13 according to the two distinct resonant scattering configurations identified above. More explicitly, for a given relative density ρ and multipole ℓ a numerical algorithm was developed adopting the following procedures: firstly, Eq. 51 is used to estimate n_{max}, the maximal number of QBS modes. For a given resonance order $0 \leq n \leq n_{max}$, the second step was to solve in β–real plane the JWKB transcendental equation (see Eq. 48) using as an initial guess the estimate in Eq. 50. Finally, in order to solve in β–complex plane Eq. 13, it was necessary to develop a subroutine based on generalized Newton's method that use the previous JWKB results as improved initial guess. In the case where the order n is greater than n_{max}, the Transmission Resonances (TR) modes can be excited. However, due to modal degeneracy, related to these resonances, the transcendental Eq. 13 was solved in β–complex plane using a generalized Muller's method where the JWKB (see Eqs. 58 and 60) estimates to TR were used as an initial guess either.

The present model does not consider the dissipative effects due to viscosity. The validity of the present results implies that the bubble radius dimension should be assumed greater than few micron meters (Urick 1948, Holdaway et al. 1999). It is known that viscosity can play a central role for bubbles of smaller radii, leading to a drastic reduction of the mean lifetime of the resonance (Urick 1948, Holdaway et al. 1999); In

this manner, a comparison between the present results with experimental data, necessarily imposes a restriction on the set of parameters where dissipative effects are most negligible. Thus, for frequencies ranging from 20kHz to 200MHz, it is assumed a scattering scenario related to an incident ultrasonic plane wave reaching bubbles with radius greater than 10μ. Experiments conducted on these lines can be found in the study of optical tweezing microbubble to observe their dynamics when submitted to ultrasound (Garbin 2006). So under these assumptions, in this present case the size parameters β varying from 10^{-1} to 10^{2} were considered. Besides, typical parameter values for water and air were adopted, where the relative density, refractive index and internal reflected critical angle θ_c are $\rho \approx 788.39$, $N \approx 4.41$ and $\theta_c \approx 13.11^{\circ}$ respectively.

In Fig. 7a, the resonant positions ($\beta_{\ell,n}$, left vertical axis) and widths ($b_{\ell,n}$, right vertical axis) for QBS and TR resonances are plotted for a resonant quadrupole ($\ell = 2$) as the resonance order n varies. It seems that even at a very low multipole order such $\ell = 2$, the resonance widths $b_{\ell,n}$ for QBS and TR are still considerably sharp as predicted by JWKB approximate results given by Eqs. (49 and 60) respectively.

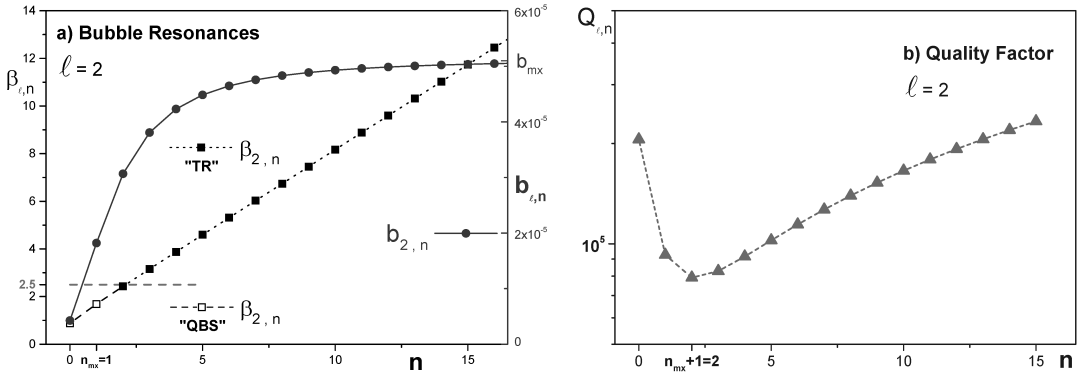

Figure 7 - For $\ell = 2$ and for several resonances orders n, shows in panel (**a**) in a double vertical axis the resonance position ($\beta_{\ell,n}$, left vertical axis) as well as the resonance width ($b_{\ell,n}$, right vertical axis), in case for Bubble's Quasi-Bound State (QBS) and Transmission (TR) Resonances. The panel (**b**) shows the behavior of the $Q_{\ell,n}$–factor as n varies.

In addition, Fig. 7a shows, as expected (see Eq. 49), that in the case of $\ell = 2$ only two ($n_{max} = 1$) QBS resonances can be excited. Besides, it may also be noted in Fig. 7a that the TR like resonances occurs only for values of $\beta_{\ell,n} \geq \ell + 1/2 = 2.5$ and the related resonance order n such that $n > n_{max}$. Besides, the left vertical axis in Fig. 7a shows that the TR like resonances widths $b_{\ell,n}$ can reach the asymptotic value b_{mx} only in the limit of geometrical acoustics, where $\beta_{\ell,n\to\infty} >> \ell + 1/2$. In addition, Fig. 7b shows for $\ell = 2$ the behavior of the quality factor $Q_{\ell,n}$ (see Eq. 56) as the resonance order n varies. It is interesting to note that $Q_{\ell,n}$ reaches a minimum value around 10^5 related to the first TR mode that occurs for $n = 2 = n_{max} + 1$. Here it is important to notice that the present results are corroborated by those reported in the pioneering work of Gaunaurd, Scharnhorst and Überall (Gaunaurd et al. 1979). At least three decades ago, these authors (Gaunaurd et al. 1979) have shown the possibility of existence of narrow *monopolar resonances* in bubbles either.

As it is shown by Eqs. (49, 60 and 51) respectively, by increasing the multipole order ℓ it is expected that sharper resonances occur and n_{max} the maximum number of QBS may rise. This is exactly found and shown

in Fig. 8a, where $\ell = 7$ and $n_{max} = 6$. In other words, when comparing Figs. 7a and 8a it is seen that n_{max} increases linearly as ℓ increases. Since by raising the angular momentum ℓ (see Eq. 27), it linearly increases the value of the impact parameter I_ℓ, which in the effective potential picture, means a deeper potential well ΔU_{eff} (see Eq. 25). As a consequence of this U_{eff} behavior, sharper resonance widths $b_{\ell,n} \approx b_{mx} \approx 5.10^{-5}$ are found even for larger values of the resonance order n as it is shown by the right vertical axis in Fig. 8a. Besides, Fig. 8b shows that $Q_{\ell,n}$ related to QBS modes vary in range from 10^{10} to 10^6 and similar to Fig. 7b, $Q_{\ell,n}$ has a minimum at $n = 7 = n_{max} + 1$ related to excitation of the first TR mode for this particular case of $\ell = 7$.

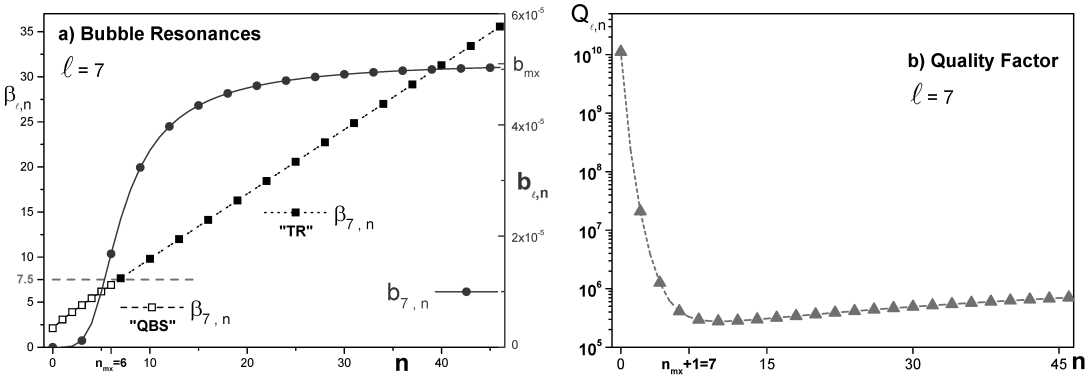

Figure 8 - Similar to Fig. 7, but for multipole $\ell = 7$ this figure in (**a**) shows as function of the resonance order n the resonance positions ($\beta_{\ell,n}$, left vertical axis) as well as the widths ($b_{\ell,n}$, right vertical axis) for the Bubble's Quasi-Bound State (QBS) and Transmission (TR) Resonances. The panel (**b**) shows the behavior of the $Q_{\ell,n}$–factor as n varies.

Moreover, the graphs in Figs. 9 and 10 show the Quasi-Degenerated Transmission Resonances for several positions $\beta_{\ell,n}$ ($\beta_{\ell,n} \geq \ell + 1/2$) and widths $b_{\ell,n}$ ($b_{\ell,n} \sim O(b_{mx})$), for a related set of resonance orders $n > n_{max}$. In Fig. 9a the behavior of the TR is analyzed in the case of even multipoles values $\ell = 2, 4, 6$. Here it is important to note the convergence proximity of the resonance positions ($\beta_{\ell+2,n} \approx \beta_{\ell,n+1} \approx \beta_{\ell-2,n+2}$), situation very similar to a quasi-degenerated energy levels in quantum mechanics picture (Schiff 1968, Griffiths 2005). Besides, Fig. 9b shows that these resonances are also considerably sharp, since $b_{\ell,n} \sim b_{mx} \approx 5.10^{-5}$. Finally, Fig. 10a for resonance positions $\beta_{\ell,n}$ and Fig. 10b for widths $b_{\ell,n}$, respectively, show that all the above mentioned Quasi-Degenerated Transmission Resonances features are also maintained when plotting TR related to the odd multipole values $\ell = 3, 5, 7$. The next section, we comment and summarize the main results of this work.

5 - CONCLUSIONS

In this paper the acoustic resonances of a spherical air bubble cavity in unbounded water (see Fig. 1a) are calculated. Above all the mathematical complexity of the difficult calculations (see Fig. 1b), a physical interpretation is needed to clarify the results. To this end, the concept of effective potential U_{eff} explicitly given in Eq. 21 (see Figs. 5 and 6) is applied according to the analogy between acoustic waves and matter waves in quantum mechanics (Nussenzveig 1969, 1992, Guimarães and Nussenzveig 1992). Within this framework, the JWKB perturbative method was employed to calculate such resonances, as well as to give

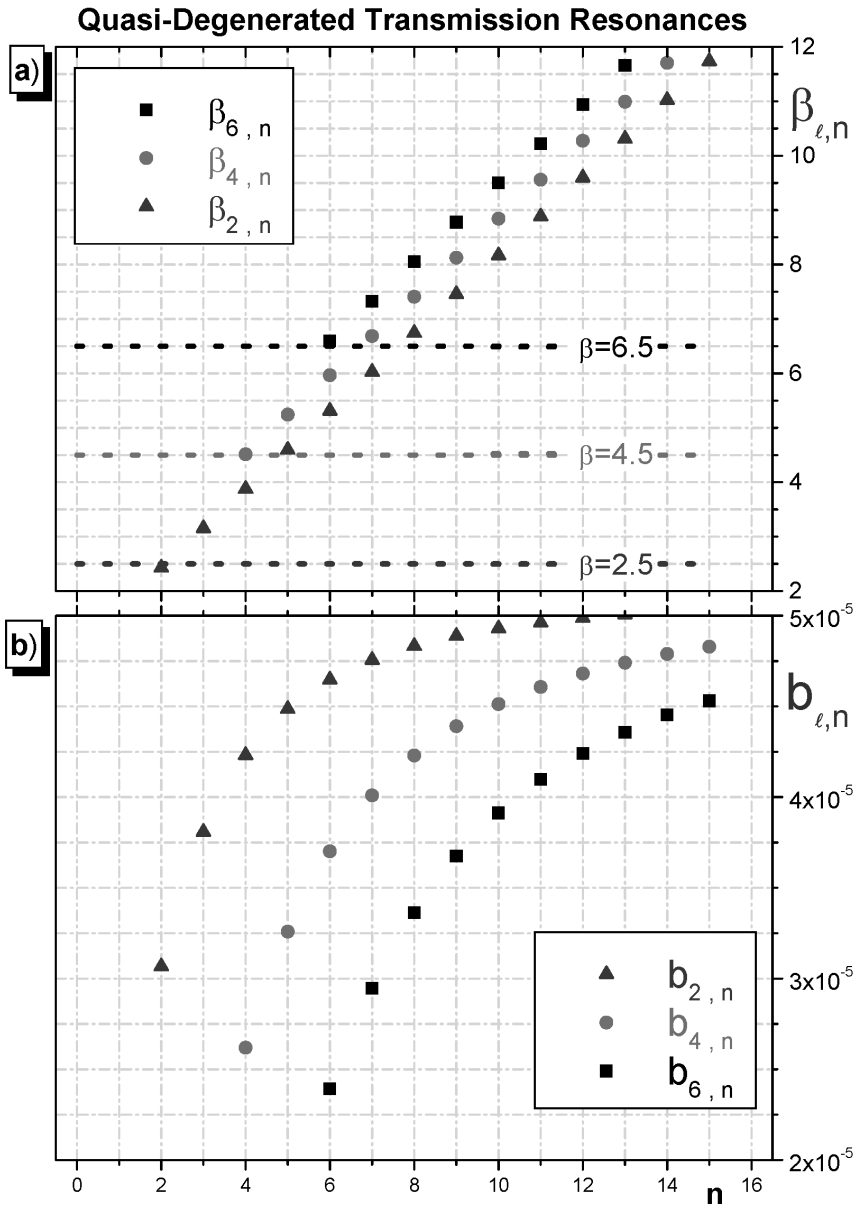

Figure 9 - For even multipoles $\ell = 2, 4, 6$, this figure shows for Quasi-Degenerated Transmission Resonances the behavior of the positions (top panel–**a**) and widths (bottom panel–**b**) as the resonance order n varies.

a physical interpretation to present results. The JWKB method is suitable for resonance calculations in asymptotic "high-energy" $(\omega/c_2)^2$ values regime. Despite of this fact, it is observed in the case of resonances calculations, that the JWKB method provides satisfactory estimates even very close to the Rayleigh regime, where the bubble radius is of the same order of the incident wavelength such that $\beta \leq \ell \approx O(1)$ (see Fig. 7a). In addition, the present results suggests that the bubble is a very robust resonant cavity with extremely high quality factor $Q_{\ell,n}$ ranging from 10^{10} to 10^5 (see Fig. 8b and Fig. 7b). Consequently, the resonant bubble

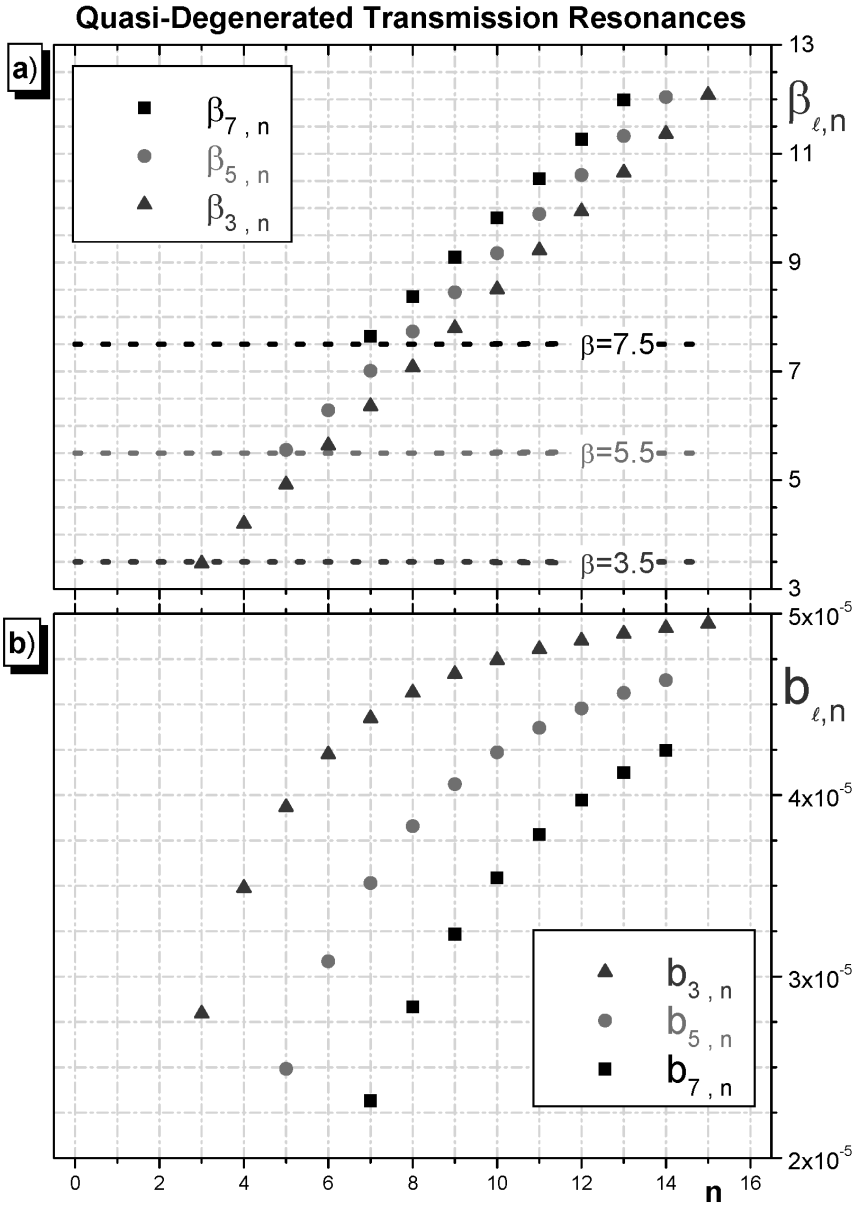

Figure 10 - Similar to Fig. 9, but for odd multipoles $\ell = 3, 5, 7$, this figure shows the behavior of positions ($\beta_{\ell,n}$, top panel–**a**) and widths ($b_{\ell,n}$, bottom panel–**b**) as function of n in the case of the Quasi-Degenerated Transmission Resonances.

can efficiently store acoustic energy during long time intervals. A time duration that is even greater than the period of its surface Minnaert oscillations (see Eqs. 55 and 64). In relation to this fact, it was observed that there are two distinct categories of bubble narrow resonance, namely: in the first case, the tunneling of the incident wave to interior of bubble can excite n_{max} QBS (Quasi-Bounded States of the sound), while in another particular situation, the incident wave can generate collectively various acoustic vibration modes analogous to the TR (Transmission Resonances) in quantum mechanics. The width $b_{\ell,n}$ of these latter type

of resonances show a particular behavior; it tends asymptotically to a constant value b_{mx} (see Figs. 7 and 8). More specifically speaking, a remarkable TR feature is the modal quasi-degeneracy (see Figs. 9 and 10), where many resonant ℓ–multipoles with same parity (odd or even values) can simultaneously vibrate inside the bubble during the mean lifetime interval τ, which in general is longer than the Minnaert bubble surface oscillation period T_M (see Eq. 64). Moreover, since the relative refractive index N is greater than unity, it is important to comment that for both TR and QBS resonances, one of the most important mechanism that supports these long resonance mean lifetimes τ is the occurrence of almost perfect internal reflection. Finally, in the present picture, it has been shown that the Minnaert oscillation can be interpreted as a broader (see Eq. 70) very low frequency Transmission Resonances (see Eq. 69 and the inequality in Eq. 65, respectively) with the shortest lifetime (see Eq. 71).

In addition, comparing laser cavities in microdroplets (Alexandr et al. 2012) with present acoustic bubbles cavities, regardless the value of the excited resonant multipole ℓ, we conclude that bubbles are more efficient in storing energy. We believe that this particular feature of the bubble is mainly due to high density contrast between air and water at bubble surface. Notice that this large value of the density gradient arises at $r = a$ an almost impenetrable potential barrier for any value of the angular momentum ℓ (see Eqs. 21, 24 and 25). In other words, we think that the bubble is an extremely robust acoustic resonant cavity due to almost total internal reflection and wave tunneling through barrier $\Delta U_{eff}(25)$, these features permit the bubble to sustain very narrow resonances (even in the case of low-order multipoles ℓ) with related high Q-factors (for instance see Figs. 7 and 8) and such resonances should be collectively quasi-degenerated. We believe that these mechanisms can take considerable amount of the incident acoustic energy and efficiently retain this energy inside the bubble during several oscillations of its surface.

Summing up, although very preliminary considerations have been treated above, the authors believe that the present results open a new perspective to a problem that has been deeply considered in many respectful works. The new results point out two different resonant regimes which may give a physical explanation to the impressive acoustic energy storage mechanism within the bubble. In addition, the present analysis can have some implications in other fundamental scientific research areas, such as the studies on a sonoluminescencing bubble (Putterman and Weninger 2000), the medical and technological developments of using an acoustic beam with a suitable frequency bandwidth to excite special resonant vibrational modes of a spherical bubble cavity (Chomas et al. 2000, Garbin 2006) as well as human made acoustic insulating metamaterials (Thomas et al. 2009, Pierre et al. 2014, Leroy et al. 2015). Besides, from the theoretical point of view, we think that this work offers to the experimental acoustician an opportunity of further exploration of the bubble resonances by considering other forms of beam incidence for resonance excitation. In order to improve the present results, our next step is to obtain a better understanding of the role of energy dissipative mechanisms such as the viscosity and the surface tension effects in bubble resonance phenomenon. More specifically, in analogy with Mie scattering in dielectric spherical drops, we know that the occurrence of very small absorptive inclusions on a droplet's surface can suppress resonances (Simão et al. 2001, 2005). So we hope that in the case of acoustic scattering by osculating microbubbles, the viscosity and the surface tension should increase the width of the resonances. Moreover, we think that during the bubble drag in the water, the surface tension cannot be strong enough to maintain the bubble shape as perfectly spherical. In this way, still making analogy with size and shape effects in Mie scattering, it is well known that in the case of light scattering by non-spherical microdroplets, due to the broken spherical symmetry, the angular momentum degeneracy is lifted and for spheroidal droplets the resonance widths increases as the aspect ratio

increases (Chýlek et al. 1995, Bambino et al. 2003, Gorodetsky and Ilchenko 1994). Summarizing, all these above effects contribute to increase the value of resonances widths, consequently the related value of the Q-factor should be less than the similar idealized case of non viscous spherical bubble. These studies are in progress and they are planned to be submitted for publication briefly.

ACKNOWLEDGMENTS

Both of us (LGG and AGS) would like to express their deep gratitude to Professor Herch Moysés Nussenzveig. He who has inspired many generations of physicists through his fundamental and advanced physics books, teachings and research advising. Actually, it is very important for us to comment that the elaboration of the present work was only made possible as a direct consequence of elucidative efforts of Prof. Nussenzveig in delving with this fine, intricate and very subtle subject of wave scattering by particles of definite geometry as well as the development of suitable analogies. In other words, it is one of the aims of the present work to pay due homage to Nussenzveig by extending the power of such analogies in physics to another area of classical phenomena, fluid mechanics. More specifically, applying the primordial framework developed by Prof. Nussenzveig, it was possible to show that evanescent wave tunneling, a universal wave phenomenon which is present both in the quantum and classical realm, occurring in light scattering by water droplets in clouds, is a fundamental component for sound radiation during the mechanical natural vibrations of a spherical bubble in water.

RESUMO

O problema tratado neste trabalho é o espalhamento ressonante do som por uma bolha de ar imersa na água. O formalismo do espalhamento acústico em ondas parciais, relacionado ao problema proposto, é revisitado. Com base na analogia entre o espalhamento de partículas na mecânica quântica e o espalhamento acústico, os modos de vibração naturais da bolha, denominados de ressonâncias, são descritos e interpretados. Dentro deste contexto, um modelo foi elaborado para descrever fisicamente a interface ar-água e as implicações do grande contraste entre as densidades nos vários regimes dos modos naturais de oscilação da bolha. Os resultados principais estão apresentados em termos dos períodos relacionados aos tempos de vida das ressonâncias e nos fatores de qualidade da cavidade. Considerando as dimensões típicas das bolhas e os comprimentos de ondas sonoras em água, foram executados cálculos numéricos esplícitos utilizando a análise assintótica. É demonstrado que os períodos de duração de vida das ressonâncias obedecem uma escala de acordo com o período de Minnaert, que é o menor tempo de vida de uma ressonância, denominado de modo de respiração da bolha. Como esperado, as ressonâncias de maior tempo de vida resultam em fatores de qualidades de cavidade Q muito expressivos que variam entre 10^{10} a 10^{5}. As descobertas teóricas aqui expressas indicam uma melhor compreensão do mecanismo de acúmulo de energia existente em um meio repleto de bolhas.

Palavras-chave: Espalhamento Acústico, Ressonâncias de Minnaert, Métodos Semi-Clássicos, Modos de Galeria de Sussurros, Espalhamentos Mie e Rayleigh.

REFERENCES

Abramowitz M and Stegun IAE. 1972. Handbook of Mathematical Functions. Dover Publications. New York, 1046 p.

Ainslie MA and Leighton TG. 2011. Review of scattering and extinction cross-sections, damping factors, and resonance frequencies of a spherical gas bubble. J Acoust Soc Am 130: 3184-3208.

Alexandr J, Karadag Y, Mestre M and Kiraz A. 2012. Probing of ultrahigh optical q-factors of individual liquid microdroplets on superhydrophobic surfaces using tapered optical fiber waveguides. J Opt Soc Am B 29: 3240-3247.

Anderson VC. 1950. Sound scattering from a fluid sphere. J Acoust Soc Am 22: 426-431.

Bambino TM, Breitschaft AMS, Barbosa VC and Guimarães LG. 2003. Application of semiclassical and geometrical optics theories to resonant modes of a coated sphere. J Opt Soc Am A 20(3): 489-498.

Blais A, Huang RS, Wallraff A, Girvin SM and Schoelkopf RJ. 2004. Cavity quantum electrodynamics for superconducting electrical circuits: an architecture for quantum computation. Phys Rev A 69: 062320.

Born M and Wolf E. 1975. Principles of Optics. Pergamon Press, Oxford, 985 p.

Bretagne A, Tourin A and Leroy V. 2011. Enhanced and reduced transmission of acoustic waves with bubble meta-screens. Appl Phys Lett 99(22): 221906-1/221906-3.

Chomas JE, Dayton PA, May D, Allen J, Klibanov A and Ferrara K. 2000. Optical observation of contrast agent destruction. Appl Phys Lett 77: 1056-1058.

Chýlek P, Videen G, Ngo D, Pinnick RG and Klett JD. 1995. Effect of black carbon on the optical properties and climate forcing of sulfate aerosols. J Geophys Res-Atmos 100(D8): 16325-16332.

Debye P. 1909. Naherungsformeln für die zylinderfunktionen für groe werte des arguments und unbeschrankt veranderliche werte des index. Math Ann 67: 535-558.

Devaud M, Hocquet T, Bacri J and Leroy V. 2008. The Minnaert bubble: an acoustic approach. Eur J Phys 29: 1263-1285.

Feuillade C and Clay CS. 1999. Anderson (1950) revisited. J Acoust Soc Am 106: 553-564.

Flax L, Gaunaurd G and Uberall H. 1981. Theory of resonance scattering. Physical Acoustics 15: Principles and Methods, Chapter 3, Mason WP and Thurston RN (Eds), Academic Press, New York, p. 191-294.

Garbin V. 2006. Optical tweezers for the study of microbubble dynamics in ultrasound. Ph. D. thesis, Universita degli studi di Trieste.

Garbin V, Dollet B, Overvelde M, Cojoc D, Di Fabrizio E, van Wijngaarden L, Prosperetti A, De Jong N, Lohse D and Versluis M. 2009. History force on coated microbubbles propelled by ultrasound. Phys Fluids 21: 092003-1/092003-7.

Gaunaurd G, Scharnhorst KP and Überall H. 1979. Giant monopole resonances in the scattering of waves from gas-filled spherical cavities and bubbles. J Acoust Soc Am 65: 573-594.

Gaunaurd G and Überall H. 1981. Physical Acoustics Vol XV: Principles and Methods Chapter 3, Mason WP and Thurston RN (Eds), Academic Press, London.

Gorodetsky ML and Ilchenko VS. 1994. High-Q optical whispering-gallery microresonators: precession approach for spherical mode analysis and emission patterns with prism couplers. Opt Commun 113(1-3): 133-143.

Griffths DJ. 2005. Introduction to Quantum Mechanics. Prentice Hall, New Jersey, 480 p.

Guimarães LG and Nussenzveig HM. 1992. Theory of Mie resonances and ripple fluctuations. Opt Comm 8: 363-369.

Hickling R and Plesset MS. 1964. Collapse and rebound of a spherical bubble in water. Phys Fluids 7: 7-14.

Holdaway GP, Thorne PD, Flatt D, Jones SE and Prandle D. 1999. Comparison between adcp and transmissometer measurements of suspended sediment concentration. Cont Shelf Res 19(3): 421-441.

Landau LD and Lifshitz EM. 1987. Fluid Mechanics, Pergamon Press, Oxford, 552 p.

Leighton T. 1994. The Acoustic Bubble, Academic Press, London, 640 p.

Leroy V, Strybulevych A, Lanoy M, Lemoult F, Tourin A and Page JH. 2015. Superabsorption of acoustic waves with bubble metascreens. Phys Rev B 91: 020301-1/020301-5.

Minnaert M. 1933. On musical air-bubbles and the sound of running water. Philos Mag 16: 235-248.

Morse PM and Ingard KU. 1968. Theoretical Acoustics, McGraw-Hill Book Co, New York, 949 p.

Nussenzveig HM. 1969. High frequency scattering by a transparent sphere: I direct reection and transmission. J Math Phys 10: 82-124.

Nussenzveig HM. 1992. Diffraction effects in semiclassical scattering, Cambridge University Press, Cambridge, 256 p.

Nussenzveig HM and Wiscombe WJ. 1987. Diffraction as tunneling. Phys Rev Lett 59: 1667-1670.

Olver PJ. 2014. Introduction to Partial Differential Equations (Undergraduate Texts in Mathematics series), Springer Verlag, New York, 635 p.

Pierre J, Dollet B and Leroy V. 2014. Resonant acoustic propagation and negative density in liquid foams. Phys Rev Lett 112: 148307-1/148307-5.

Prosperetti A. 1984. Bubble phenomena in sound fields: Part one. Ultrasonics 9: 69-77.

Putterman S and Weninger KR. 2000. Sonoluminescence: how bubbles turn sound into light. Annu Rev Fluid Mech 32: 445-476.

Rayleigh L. 1917. On the pressure developed in a liquid during the collapse of a spherical cavity. Philos Mag S 6 34(200): 94-98.

Schiff LI. 1968. Quantum Mechanics, McGraw-Hill, New York, 432 p.

Shew W. 1994. Waves and Fields in Inhomogeneous Media, IEEE Press on Electromagnetic Waves, New York, 608 p.

Simão AG, De Mendonça JP, Santiago RB, De Moraes PC, Soares PC and Guimarães LG. 2005. Narrow resonances and ripple fluctuations in light scattering by a spheroid. Appl Optics 44(16): 3370-3376.

Simão AG, Guimarães LG and Videen G. 2001. A comparative study in resonant light scattering between spherical and cylindrical dielectric hosts with a metallic inclusion. J Quant Spectrosc Ra 70(4-6): 777-786.

Stride E and Saffari N. 2003. Microbubble ultrasound contrast agents: a review. Proc Instn Mech Engrs 217: 429-447.

Strybulevych A, Leroy V, Shum AL, Koksel HF, Scanlon MG and Page JH. 2012. Use of an ultrasonic reflectance technique to examine bubble size changes in dough. IOP Conf. Series: Material Science and Engineering 42: 012037-1/012037-4.

Thomas DH, Looney P, Steel R, Pelekasis N, McDicken WN, Anderson T and Sboros V. 2009. Acoustic detection of microbubble resonance. Appl Phys Lett 94: 243902-1/243902-3.

Thomas EL. 2009. Bubbly but quiet. Nature 462: 990-991.

Urick R. 1948. The absorption of sound in suspensions of irregular particles. J Acoust Soc Am 20(3): 283-289.

Watson GN. 1944. Theory of Bessel Functions, Cambridge Univ. Press, Cambridge, first published 1922, sec. edit, 820 p.

Zinin PV and Allen III JS. 2009. Deformation of biological cells in the acoustic field of an oscillating bubble. Phys Rev E 79(2): 021910-1/021910-12.